

Participant-like scaling behavior of multiplicity and charged hadron spectra in relativistic heavy ion collisions.

R. S. Hollis,¹ A. Iordanova,¹ and D. J. Hofman²

¹*University of California, Riverside, CA, 92521*

²*University of Illinois at Chicago, Chicago, IL, 60607*

(Dated: June 16, 2018)

We present a method for parameterizing the charged particle multiplicity and charged hadron spectra from heavy ion data with a simple, Glauber-inspired, model. The basis of this model is derived from the observation of leading hadrons in pp collisions and the number of interactions calculated by a Glauber model. Singly hit and multiply hit nucleons are treated as different sub-components of the same collision. With this scheme, for fixed sub-component yields, we find that the multiplicity and charged hadron spectra can be reproduced, without the need for large suppression at high- p_T . Suppression is still observed, in the low- to intermediate- p_T region, but this is confined to suppression of surface emission partons. At high- p_T , the suppression disappears entirely, leaving only a possible Cronin-type enhancement. The suppression observed in 200 GeV collisions is found to be the same for 62.4 GeV data.

INTRODUCTION

The comparison of hadronic collider (pp collisions) and electron collider ($e^+ + e^-$ collisions) data have shown a clear discrepancy in the produced particle multiplicity for collisions measured at the same center-of-mass energy. This has long been explained by the observation that hadronic interactions can be decomposed in terms of “collision products” and “leading hadrons” – with the latter carrying away (on average) half of the total energy available for particle production [1]. It is found that one can unify these data by shifting the center-of-mass energy of the pp collisions to an effective center-of-mass energy, which is half of the original collision energy, empirically determined. Superimposing central heavy ion data onto this agrees more closely with the $e^+ + e^-$ data than the hadronic collision (pp) data [2]. Combining all these observations, one can surmise that collisions in which all “constituents” of the proton are used (i.e. no leading hadron) will produce higher ($e^+ + e^-$ -like) multiplicities.

The model presented here, originally described in Ref. [3], uses these ideas as a premise to divide the participant region in heavy ion collisions into two distinct regions; these are noted as “mono” and “multi”. A Glauber model [4] is used to calculate the number of participants and the number of times each nucleon is struck by another from the opposing nucleus. Mono refers to nucleons which undergo a single hit – similar to pp interactions, which presumably can “liberate” a leading hadron. Multi refers to nucleons which are multiply struck (by two or more) nucleons, however, these are only counted once and thus do not accumulate as quickly as the number of binary collisions.

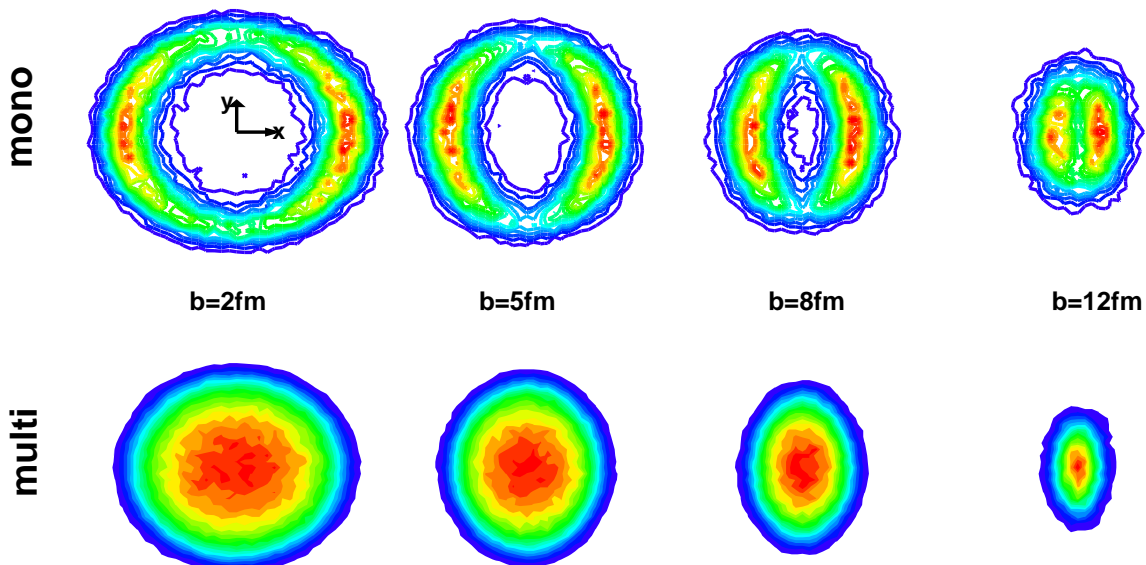


FIG. 1. (color online) Predicted relative positions of mono- (upper) and multi-collisions (lower). The distributions are based on a Glauber calculation at impact parameter $b=2, 5, 8, 12$ fm ($N_{\text{part}} \sim 359, 261, 140, 24$, $N_{\text{mono}} \sim 28, 38, 33, 12$, and $N_{\text{multi}} \sim 331, 223, 107, 12$). In this picture, the reaction plane is always along the x -axis.

This phenomenological approach is similar to the successful core/corona approach of EPoS [5]. The main technical difference surrounds the expected position with respect to the reaction plane, of the mono (or corona) nucleons. The current model expects that the peak of mono nucleons to be *along* the reaction plane (see Fig. 1), whereas in the corona from EPoS is expected to peak 90° away [5]. A more recent ‘toy model’ implementation by the EPoS authors [6], however, does use the same “Glauber-method” to determine core (multi) and corona (mono) regions to describe the strangeness enhancement observed in Au+Au and Cu+Cu data. In that implementation no interactions between the core and corona regions is assumed, each “corona” contributes one-half of a minimum bias interaction. The authors note that fixing the mono (corona) is not necessary. However, although they undergo different assumptions, both can provide a good description of the data. Where these models differ is in the extent to which they can be (or at least have been) applied and the possible origin of the two components, or regions, of the collision. By using the model presented here, it is possible to not only describe with success low- p_T phenomenon observed in heavy ion collisions but also high- p_T phenomena. This can lead to hints as to the origin of disappearing back-to-back jets and their reappearance at low- p_T .

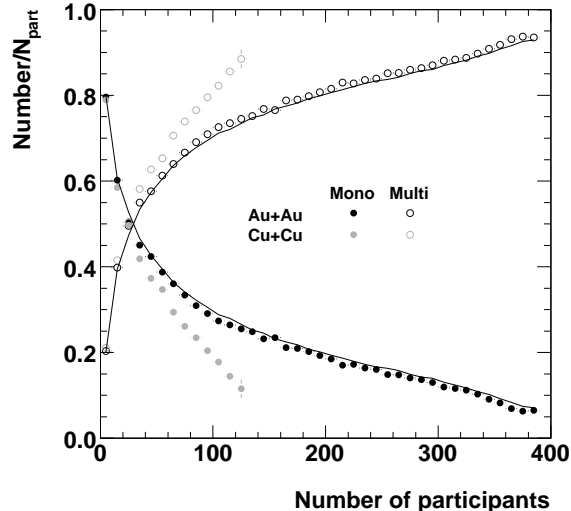


FIG. 2. The relative number of mono and multi collisions versus the number of participants. Black (grey) circles represent Au+Au (Cu+Cu) collisions at 200 GeV ($\sigma_{NN} = 42$ mb); closed and open symbols represent mono and multi collisions respectively. The values for 19.6 GeV ($\sigma_{NN} = 33$ mb) Au+Au data are depicted as lines for comparison.

THE MODEL

The implementation of this model is very simple. A Glauber model is used to count the number of times each nucleon is struck (the Glauber model implementation is similar to Ref. [7]). For each Monte-Carlo “collision” the nucleons are sorted into three categories: not hit (spectators), singly hit nucleons (N_{mono}), and multiply hit nucleons (N_{multi}). Spectators are not considered in this model. After many trials, and at all possible impact parameters, the average number of mono- and multi-assigned nucleons are calculated. Figure 2 illustrates the mean N_{mono} and N_{multi} found for Au+Au (black circles) and Cu+Cu (grey) collisions at $\sqrt{s_{NN}} = 200$ GeV. N_{mono} and N_{multi} versus centrality are not found to appreciably change with collision energy, as shown by lines depicting N_{mono} and N_{multi} for 19.6 GeV collisions.

After calculating the number of mono and multi participants for a given centrality class it is possible to form the multiplicity (and spectra, etc.) corresponding to that data using the formula:

$$Y_{\text{Au+Au}} = N_{\text{mono}}Y_{\text{mono}} + N_{\text{multi}}Y_{\text{multi}} \quad (1)$$

$Y_{\text{Au+Au}}$ represents the modeled Au+Au data, Y_{mono} is the yield expected from singly interacting nucleons (ostensibly minimum bias pp data) and Y_{multi} is the yield expected from the multi underlying distribution. Y_{mono} and Y_{multi} are fixed for a given data sample and do not change versus centrality. Y itself represents any distribution, for example multiplicity, charged hadron spectra, kinetic freeze-out temperature, or any other observable.

In this paper, we first explore the possible origin of the underlying multi distribution which could be from one of many different sources such as non-single diffractive (NSD) events (unlikely as these may still have leading hadrons), high-multiplicity events (for example greater than $\langle N_{\text{ch}}^{pp} \rangle / 2$), high- p_T data ($\hat{p}_T > \sim 1.8$ to represent the close-packedness of the multi nucleons), a gluon-only source distribution. We use each of these different hypotheses to test the systematic dependence – although not to choose a preferential particle production mechanism but rather to provide a proof of principle that one can reasonably reproduce the particle distributions in heavy ion collisions from these simple sources. We note that a single distribution for mono (pp minimum bias) and a single distribution for multi is assumed, which is sufficient to reproduce all the data versus centrality. The centrality dependence observed in the data is then entirely due to the interplay between N_{mono} and N_{multi} , Fig. 2, and not from a changing or modified underlying distribution.

Secondly, as a more rigorous test, fits to the data to extract the underlying mono and multi distributions will be made. In fact this is necessary to analyze more exotic data than multiplicity and charged hadron spectra. In this way we decouple ourselves from (for example) PYTHIA [8] to describe the detailed identified particle spectra. By using Eqn. 1 and the measured data to simultaneously extract the underlying distributions, both the modification to the

pp minimum bias collisions at the surface (mono) as well as the true underlying multi distribution can be studied. As Glauber has no recourse to produce particle distributions, this model has a purely phenomenological approach to describe the heavy ion experimental data.

One important distinction to note for the current model versus many other two-component models is the absence of “collision scaling”. Other two-component models assert that one component factorizes with the number of participants (usually associated with soft particle production), and the second with the number of nucleon-nucleon interactions (N_{coll} – representing hard collisions) within the collision [9–12]. In the current discussion, we assert that the number of collisions is not the correct scaling variable. If, as is hypothesized, upon collision the system becomes a hot, dense QCD matter then it may become difficult to reliably count individual nucleon-nucleon collisions. The currently accepted approach used to validate the number of collisions is to measure the spectrum of direct-photons in $A+A$ collisions, relative to that in pp interactions. As the direct photons are not expected to interact with the medium, it is assumed that the measured $R_{AA} = 1$ validates the use of N_{coll} [13], illustrating that the number of originally produced photons are consistent with pp . In more current data, however, the previously observed N_{coll} scaling at $p_T \sim 6 \text{ GeV}/c$ is not seen at higher momenta [14], even though punch-through high- p_T hadrons are seen to escape the medium [15]. Here, we set this N_{coll} scaling assumption aside. The number of mono and multi collisions in the current model is less susceptible to the assumptions needed in order to count the number of collisions, where our *number* reflects an interaction volume (multi) and simply the number of expected nucleon-nucleon scatterings on the surface (mono).

For a low number of participants ($N_{\text{part}} < 25$), the number of mono collisions exceeds that of multi, and vice-versa for a high N_{part} . However, as shown in Fig. 2, the number of mono does not fall to zero even for the most central events where approximately 7% of the participants undergo only a single interaction. An important consequence in these calculations is that the sum of mono and multi, by definition, is fixed to be N_{part} . This restricts the growth of multi, unlike the rapidly growing number of binary collisions, and results in multi (and mono) being more closely associated to a “participant” variable. In calculating the mono and multi, it is found that there is a strong dependence on the collision species, in contrast to the number of binary collisions (N_{coll}) which is essentially the same at the same N_{part} . Similarly, only a weak dependence on the collision energy (inelastic pp cross-section) is observed over the energy range of the RHIC data, whereas a strong binary collision dependence on N_{coll} is noted.

MULTIPLICITY DISTRIBUTIONS

As the premise of this model uses the charged particle multiplicity to argue for distinct mono/multi regions of the collision volume it is natural to begin with a discussion of that experimental data. Here, one can simply use the measured pp distribution as the mono and a second underlying distribution (for example taken from PYTHIA) to represent the multi. We combine the mono/multi distributions (and similarly for the next section) as:

$$\frac{dN_{ch}^{\text{Au+Au}}}{d\eta} = N_{\text{mono}} \frac{dN_{ch}^{\text{mono}}}{d\eta} + N_{\text{multi}} \frac{dN_{ch}^{\text{multi}}}{d\eta} \quad (2)$$

where N_{mono} and N_{multi} distributions for Au+Au collisions are given in Fig. 2. One can hypothesize that $dN_{ch}^{\text{mono}}/d\eta$ be $dN_{ch}^{pp}/d\eta$ (i.e. precisely from minimum bias pp interactions) or it can be a free parameter in the fit. For simplicity in this first case, we assume the former; later, the latter is used to test for any modification of the underlying mono distributions.

Figure 3 shows the result of using this formalism with several hypothesized multi multiplicity distributions for Au+Au collisions at $\sqrt{s_{\text{NN}}} = 200 \text{ GeV}$. For the shown centrality bins from PHOBOS [16], one can see that the model provides a reasonable description of the data. Remember that the same underlying distributions are used for both panels, only N_{mono} and N_{multi} are changed. This is not too surprising as the basic premise of this model is to reproduce the centrality dependence of the charged particle multiplicity in the context of an absence of leading hadrons in the multi region. From this, judging the model’s success is really only dependent on the choice of the underlying multi distribution. Three simple pp multiplicity-like distributions are used for the multi component, for comparison. The pp collisions at $\sqrt{s_{\text{NN}}} = 200 \text{ GeV}$ minimum bias distribution is used (closed circles) which is similar to the “Wounded Nucleon Model” [17] approach and yields a multiplicity which is $\sim 30\%$ lower than the measured Au+Au data. Rejecting the single diffractive events yields a higher multiplicity (open circles) but is still significantly lower than the Au+Au distributions. A more radical approach is to only choose the highest multiplicity pp events, in this case more than the average (>24) (squares), which does achieve the desired multiplicity. One can understand this approach in terms of the origins of the model – as higher multiplicity events typically have lower energy leading hadrons, thus releasing more energy to particle production.

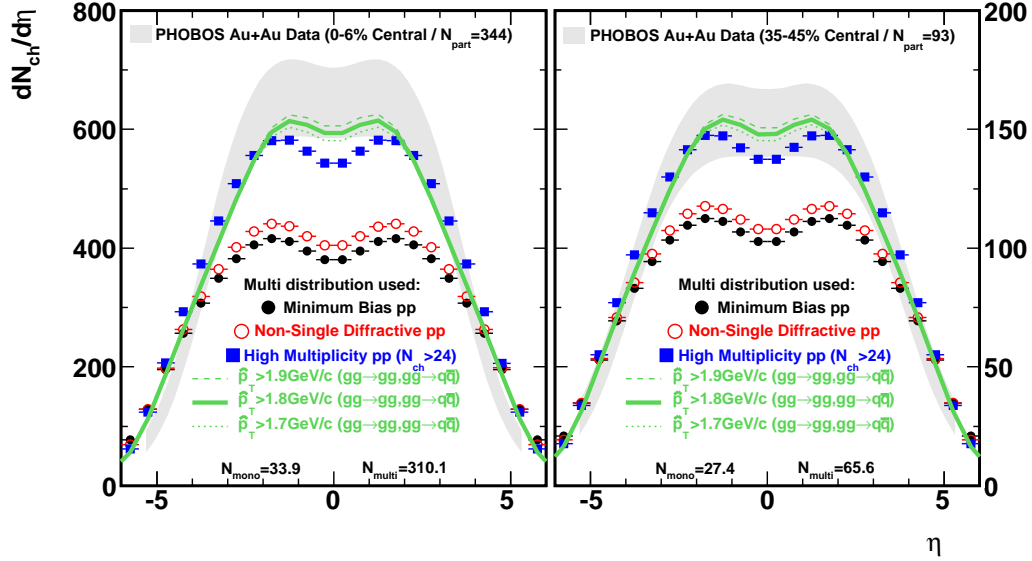


FIG. 3. (color online) Comparison between measured multiplicity versus η (PHOBOS $\sqrt{s_{NN}} = 200$ GeV Au+Au data [16]) (band) and model predictions with various candidates for the underlying “multi” $dN_{ch}^{\text{multi}}/d\eta$ distribution as noted in the legend. 0-6% central (left) and mid-central 35-45% (right) data are shown. In each model representation, the “mono” is fixed to the inelastic pp distribution at the same energy, i.e. $dN_{ch}^{\text{mono}}/d\eta = dN_{ch}^{pp}/d\eta$. Note the y -axis scale difference in each figure.

Changing the reference pp multiplicity is not the only way to alter the resultant multiplicity distribution. Also shown are a subset of events from the minimum bias pp cross-section which exclusively selects out gluon interactions ($gg \rightarrow gg$ or $gg \rightarrow q\bar{q}$) with a large momentum transfer ($\hat{p}_T > 1.8 \pm 0.1$ GeV/ c) (lines). (Note that the same multiplicity enhancement is also found by using all (quark and gluon) interactions with $\hat{p}_T > 1.8$ GeV/ c .) Such an approach may represent the close-packedness of the nucleons which may facilitate a large momentum transfer. The different minimum \hat{p}_T values used as the multi component (denoted as dotted and dashed lines in Fig. 3) show the sensitivity of the choice of \hat{p}_T in the final distribution ($dN_{ch}^{\text{Au+Au}}/d\eta$ of Eqn. 2); for multiplicity this is small.

Rather than assuming a given Y_{mono} and/or Y_{multi} multiplicity distribution, Eqn. 1 can be used to extract these two underlying distributions from the data. Two bins in centrality (preferably far apart in centrality) are used to simultaneously extract Y_{mono} and Y_{multi} . This is referred to as the pair fit method. After finding the underlying distributions, these are fixed and all centrality bins are recombined using the N_{mono} and N_{multi} as in Eqn. 1. To test the sensitivity to the bins chosen, several combinations are made. The top panels of Fig. 4 show the PHOBOS data (grey bands) with the fit distributions (solid lines). Panels (a,b), (c,d), (e,f), (g,h) in Fig. 4, show data for Au+Au collisions at 200 [16], 130 [18], 62.4 [19], and 19.6 GeV [20] respectively. In each case, the model uses the most central 0-6% and 35-45% (mid-central) data to extract the underlying mono and multi distributions. Using other bin combinations does not significantly alter the resultant distributions. The lower panel of Fig. 4 shows the underlying Y_{mono} (dashed line) and Y_{multi} (solid line) distributions from the fit. The grey and open bands represent the systematic error of the data. For comparison, the gluon-only distribution selected from PYTHIA (dot-dashed lines for the $\hat{p}_T > 1.8$ GeV/ c distribution only at 200 GeV) along with the minimum bias at the same center-of-mass energy (circles) are also shown. The underlying multi distribution is considered “stable” in the sense that using different centrality pairs does not change appreciably the extracted Y_{multi} distribution. Mono, however, is less stable when using the pair fit method and is found to be more dependent on the choice of centrality bin. Several interesting artifacts of the fit are observed. First, the extracted Y_{multi} distribution is close to that which would be obtained by using a gluon-only pp distribution in Eqn. 2, but with more yield at mid-rapidity and also narrower. Second, the mono distribution is considerably lower at mid-rapidity than the measured minimum bias pp collisions [21, 22], as shown by the comparison of the mono-collisions from the pair fit to minimum bias pp in Fig. 4, panels (b), (f), and (h). This is possibly hinting that a modification exists, due to an opaque multi region. A more detailed description of this modification is discussed in the next section. The final notable observation is that the yield of the extracted mono interactions is higher at forward rapidities, as compared to the minimum bias pp . This could possibly point to an influence of spectators in the measured data. To reiterate, Y_{multi} represents the multiplicity per participant pair of

the multi region, which is consistent with the expected yield from a gluon-dominated collisional center. The core is found to be opaque, with some of the multiplicity from the surrounding mono collisions absorbed. Importantly, even though the size of the central multi region changes, the yield per participant does not change.

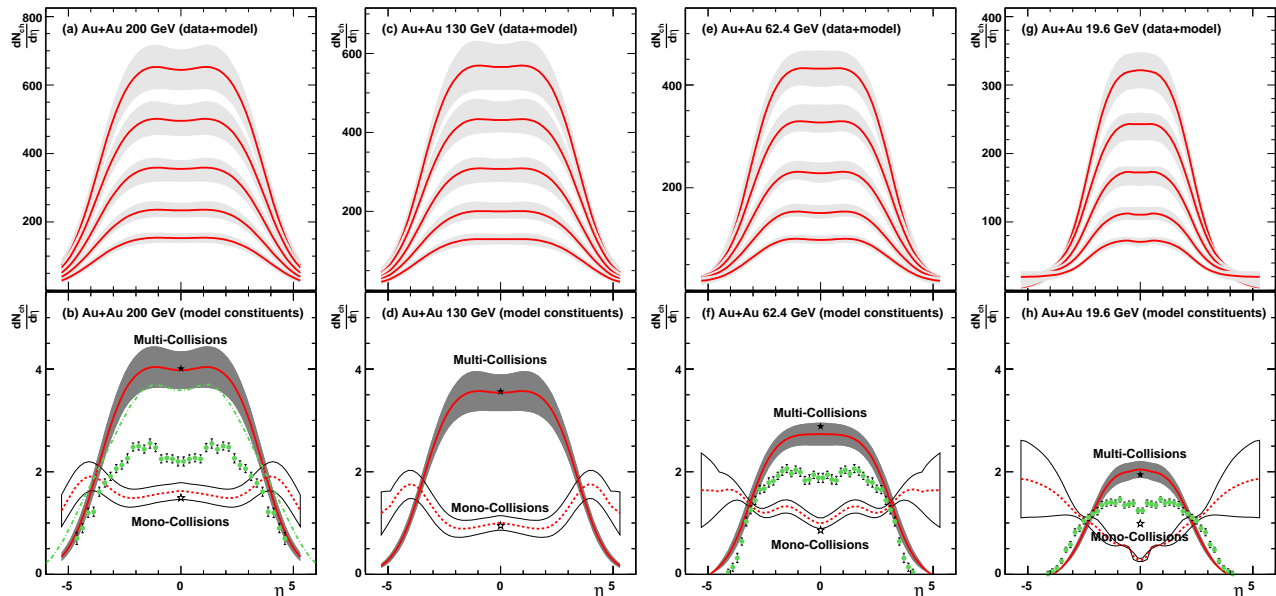


FIG. 4. (color online) PHOBOS multiplicity data (bands) from Au+Au collisions compared to the multiplicity distributions derived from the model, lines, using the pair fit method (upper panels). Panels (a,b), (c,d), (e,f), (g,h) show data for Au+Au collisions at 200 [16], 130 [18], 62.4 [19], and 19.6 GeV [20] respectively. The lower panels show the underlying Y_{mono} (dashed line/open band) and Y_{multi} (solid line/filled band). For reference, the minimum bias pp data [21, 22] (green closed circles) and gluon only distribution (green dot-dashed line) are shown (the latter for 200 GeV only). The open (closed) star symbols represent the result from the least- χ^2 method to determine the underlying mono (multi) from mid-rapidity data, see Fig. 5.

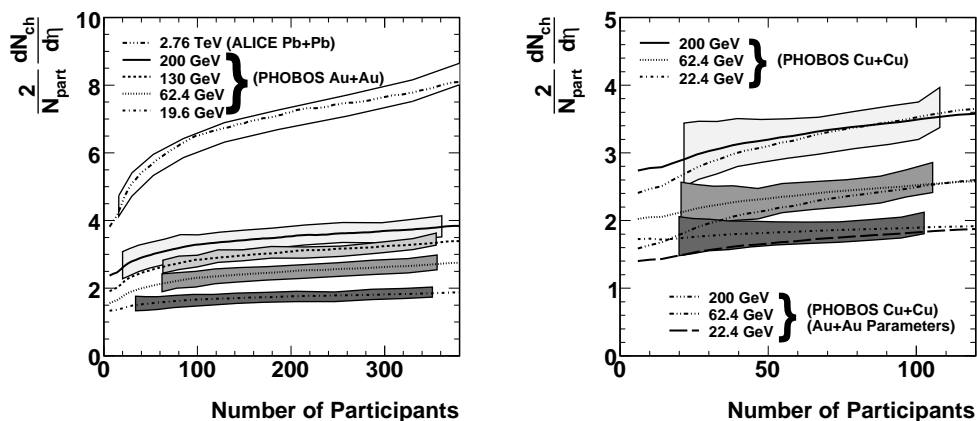


FIG. 5. PHOBOS [19, 23–25, 27] and ALICE [26] multiplicity data at mid-rapidity compared to that derived from the fit, using the least- χ^2 method, for Au+Au (Pb+Pb) data in the left panel and Cu+Cu data in the right panel. Fits are shown for RHIC energies $\sqrt{s_{\text{NN}}} = 200$ GeV (lightest grey band), 130 GeV (light grey, Au+Au only), 62.4 GeV (dark grey), and 19.6 GeV (22.4 GeV for Cu+Cu) (darkest grey). The ALICE data (2.76 TeV) are shown as a no-fill outline. For comparison, in the right panel, the expected Cu+Cu data are shown using the Y_{mono} and Y_{multi} yields found from the fits to the Au+Au collision data at the same energy. (Note that the 22.4 GeV Au+Au reference is scaled by 1.04 to account for the small difference in collision energy.) This least- χ^2 fit is a different approach than the pair fit method used above.

There is another way to extract the Y_{mono} and Y_{multi} yields from the data. Figure 5 (left panel) shows the mid-rapidity Au+Au data from PHOBOS [19, 23–25] and Pb+Pb data from ALICE [26] data (bands) together with a least- χ^2 fit (lines) using the N_{mono} and N_{multi} distributions from Fig. 2. The right panel of Fig. 5 shows the Cu+Cu data from PHOBOS [27] along with fits using that data and the extracted parameters from the fit to the Au+Au collision data at the same energy. (Note that the 22.4 GeV Au+Au reference is scaled by 1.04 to account for the small difference in collision energy.) This least- χ^2 fit is a different approach than the pair fit method used above.

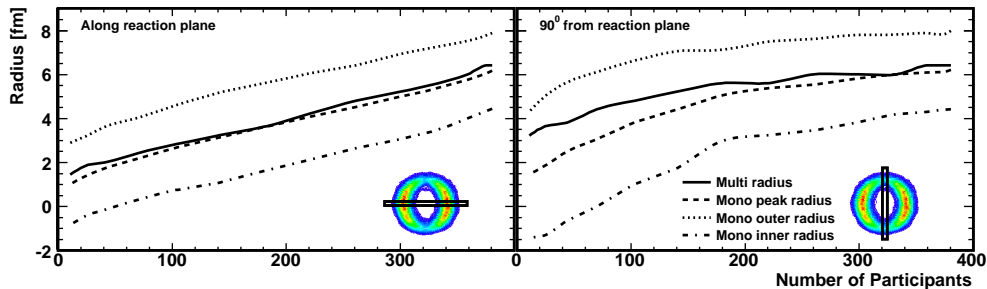


FIG. 6. (color online) Mean mono and multi radii – estimated from the Glauber model. The left (right) panel shows the radii along the (90° to) reaction plane (the line along the nuclei centers – x - (y -) axis in Fig. 1). The solid line shows the multi radius (defined as 10% of the peak). The different dashed lines represent the mono peak position (dash) and the outer/inner radius, defined as 10% of the peak yield. Negative radii (in the inner radius) represents the point at which the mono are no longer distinctly separated by the multi – i.e. mono collisions occur at every point throughout the collision area.

TABLE I. Mono and multi yields (and relative to data pp inelastic yields [21, 22, 24, 25]) as derived from the least- χ^2 fit to the mid-rapidity data from PHOBOS (Au+Au and Cu+Cu) and ALICE (Pb+Pb).

Energy (GeV)	Au+Au				Cu+Cu			
	$dN_{ch}^{mono}/d\eta$ yield	yield/ pp	$dN_{ch}^{multi}/d\eta$ yield	yield/ pp	$dN_{ch}^{mono}/d\eta$ yield	yield/ pp	$dN_{ch}^{multi}/d\eta$ yield	yield/ pp
2760	1.35	–	8.55	–	–	–	–	–
200	1.49	0.65	4.01	1.75	2.07	0.91	3.83	1.67
130	1.04	0.46	3.56	1.74	–	–	–	–
62.4	0.86	0.45	2.88	1.50	1.58	0.82	2.75	1.43
19.6	0.99	0.78	1.94	1.52	1.53	1.20	1.98	1.56

This enables the full centrality dependence of the mid-rapidity results to be simultaneously utilized and reduces the dependence of the results from the single pair choice. The resultant least- χ^2 fit at each energy well represents the data, even over two orders of magnitude of collision energy. The derived mid-rapidity mono and multi multiplicities are summarized in Table I. For comparison, these yields are shown as a star symbol to compared to the pair fit method in Fig. 4.

In an attempt to reconcile the difference between the minimum bias pp data and the derived underlying mono-distribution, we compare the detailed spacial positions of the mono and multi interactions, similar to those shown in Fig. 1. Figure 6 shows the mean radius of the multi (solid line) and mono (dot and dot-dashed lines) defined at 10% of the peak. The center of the mono (peak) is shown as the dashed line, which coincides with the multi radius. The left (right) figures show the radii along (90° to) the reaction plane. Clearly, half of the mono distribution resides within the multi distribution. One could well imagine that if the multi represents an opaque medium, then much of the mono inside the multi region could be absorbed (or at least modified/suppressed). Similarly, those outside the multi region may be suppressed should the particles be headed toward the multi region, an eclipse-type effect.

One can test the model by using the Cu+Cu data [20] to extract new Y_{mono} and Y_{multi} yields from the data and compare those to the Au+Au underlying mono and multi distributions. Figure 7 shows a similar analysis as described above for the pair fit method, this time with Cu+Cu collisions at $\sqrt{s_{NN}} = 200, 62.4,$ and 22.4 GeV. For completeness, the underlying Y_{mono} and Y_{multi} distributions from Au+Au collisions (blue dashed lines) are also used to form the multiplicity data. In comparing the underlying mono and multi distributions from Cu+Cu data to those from Au+Au data, we find that the multi distributions are very similar and that the mono distribution in Cu+Cu more closely resembles that from minimum bias pp interactions. Similarly in the right panel of Fig. 5, the same least- χ^2 method used for Au+Au collisions is applied to the mid-rapidity Cu+Cu data from PHOBOS [27] where the same trends are observed in terms of the underlying distributions.

UNIDENTIFIED CHARGED HADRON SPECTRA

Following the success of the analysis of the charged particle multiplicity, we apply this approach on more detailed data to check whether a reasonable agreement could be found. First, the unidentified charged hadron spectra versus transverse momentum (p_T) is used. This covers a different kinematic region than the low- p_T dominated multiplicity.

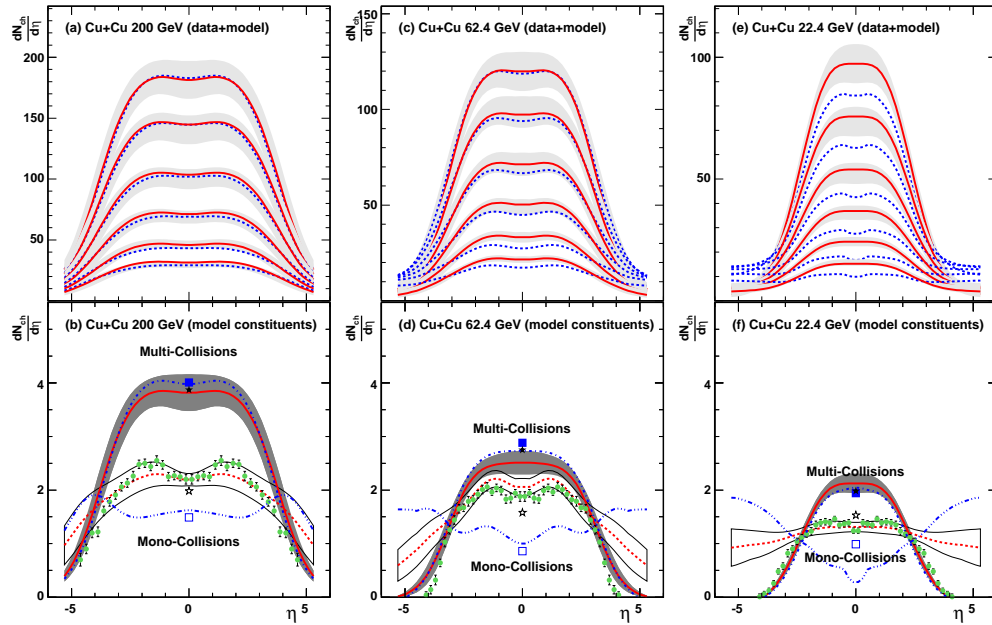


FIG. 7. (color online) PHOBOS multiplicity data from Cu+Cu collisions [20] compared to the multiplicity distributions derived from the model, using the pair fit method (upper panels, red) and from using the underlying Y_{mono} and Y_{multi} distributions from Au+Au collisions (blue, see Fig. 4). Panels (a,b), (c,d), and (e,f) show data for Cu+Cu collisions at 200, 62.4, and 22.4 GeV respectively. The lower panels show the underlying mono (dashed line/open band) and multi (solid line/filled band) extracted from the Cu+Cu data. The minimum bias pp data [21, 22] (green circles) and the underlying mono and multi distributions from the Au+Au analysis (blue dashed lines) are shown for reference. The star (square) symbols represent the least- χ^2 fit to the mid-rapidity Cu+Cu (Au+Au) data, see Fig. 5 right (left) panel.

The suppression of high- p_T particles in central events is a fascinating phenomena which has been modeled by many different theories, which are generally decoupled from the low- p_T region. Here, the full p_T range of the data is used with the primary goal of a qualitative description of the data. As an initial test, the Y_{mono} and Y_{multi} are again taken from PYTHIA, at a collision energy of 200 GeV, with mono derived from a truly minimum bias sample and multi from several hypothesized distributions as described above. Again, N_{mono} and N_{multi} are from Fig. 2.

Figure 8 shows the nuclear modification factor, R_{AA} – see Eqn. 3, for Au+Au collisions at $\sqrt{s_{\text{NN}}} = 200$ GeV for two centrality bins as measured by PHENIX [28]. It can be clearly seen that, although the model distributions do not match the experimental data precisely, the qualitative features of the data are reproduced. Using the pp minimum bias (circles) or high multiplicity (squares) simulations for the multi component of the hadron spectra do not represent the data enhancement in the intermediate p_T region with either of these as the underlying multi distribution. The minimum bias result, in this case, represents a simple visual scale of the number of collisions.

$$R_{AA} = \frac{1}{N_{\text{coll}}} \frac{d^2 N^{\text{Au+Au}}}{dy dp_T} \bigg/ \frac{d^2 N^{pp}}{dy dp_T} \quad (3)$$

$$R_{AA}^{N_{\text{part}}} = \frac{1}{N_{\text{part}}} \frac{d^2 N^{\text{Au+Au}}}{dy dp_T} \bigg/ \frac{d^2 N^{pp}}{dy dp_T} \quad (4)$$

Applying a minimum \hat{p}_T cut of 1.8 GeV/c on the minimum bias sample (dot-dashed line) results in a clear peak close to the minimum cut (as expected) but over predicts the higher- p_T data. Removing all quark interactions, leaving a gluon dominated system (solid, dotted, and dashed lines) both reproduces the intermediate- p_T peak and the lower yield at higher- p_T . To emphasize again, the objective of this analysis is not to *find* the underlying distribution, but to show that a simple underlying distribution could exist which can describe the features observed in heavy ion data.

Using the same technique to fit the data as described above for the multiplicity ‘pair fit’, charged hadron spectra can be modeled using PHENIX data [28]. The fit is performed twice, once using the 0-10% and 60-70% cross-section

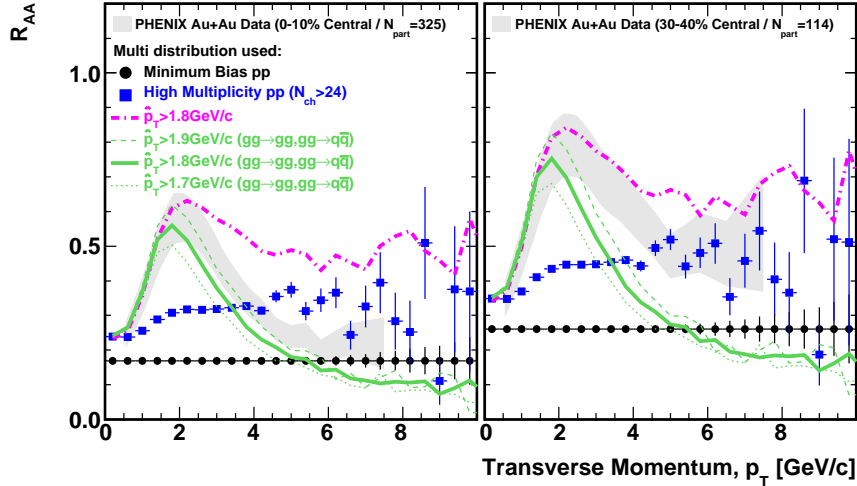


FIG. 8. (color online) Comparison between measured nuclear modification factor, R_{AA} , versus p_T (PHENIX data [28]) (band) and model predictions with various candidate Y_{multi} distributions (colored symbols) as noted in the legend. 0-10% central (left) and mid-central 40-50% (right) data are shown. In each model representation, Y_{mono} is fixed to minimum bias pp from PYTHIA.

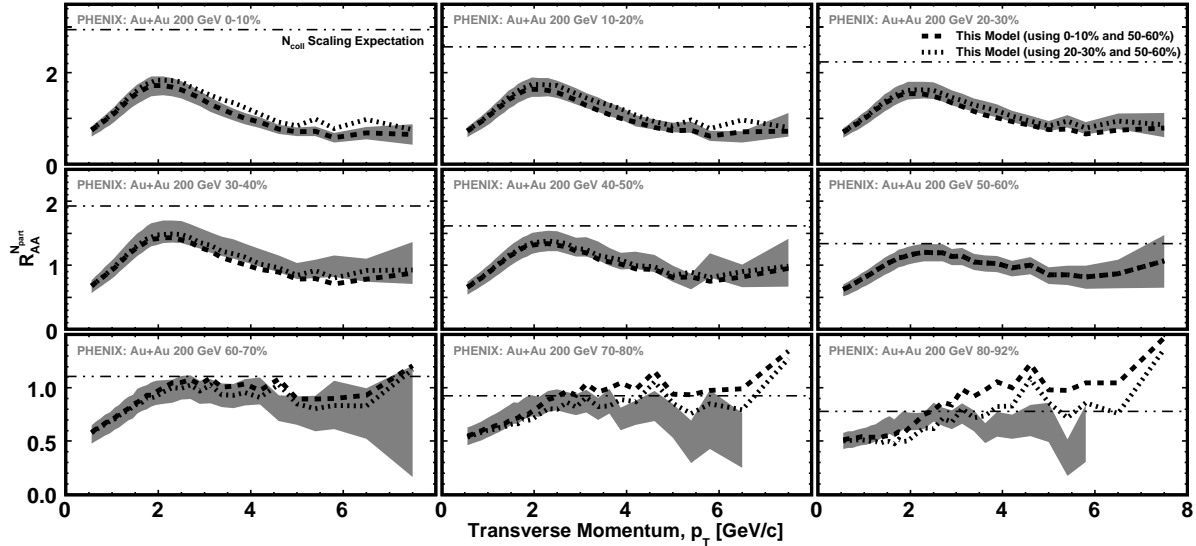


FIG. 9. Nuclear modification factor (scaled by N_{part} not N_{coll}) for unidentified charged hadrons from PHENIX [28] (filled band) at $\sqrt{s_{NN}} = 200$ GeV. The lines are the $R_{AA}^{N_{\text{part}}}$ reconstituted from the underlying mono- and multi-distributions using the pair fit method; dashed (dotted) lines use centrality bins 0-10% (20-30%) and 60-70%. In each figure, the dot-dashed line represents the expected N_{coll} scaling, assuming particle production scales as $pp \times N_{\text{coll}}$.

bins as the data pair to obtain the Y_{mono} and Y_{multi} distributions and a second pairing of 20-30% and 60-70% to test the sensitivity in the choice of centrality bins, see Fig. 9. The extracted underlying mono and multi distributions are then used to model $R_{AA}^{N_{\text{part}}}$, Eqn.4, in the remaining centrality bins.

We find that all multi-dominated centrality bins are well reproduced from the underlying mono and multi distributions using any two bins; the results are not sensitive to the choice of centrality bins. In each figure, the double-dot dashed line represents the ‘ N_{coll} ’ scaling. For data presented as R_{AA} , the line would be exactly at unity and the data yield (at high- p_T) would represent the apparent suppression. Within the mono/multi framework, we find that suppression at high- p_T is not necessary to describe the data. The most peripheral bins, perhaps, are not as well described. An explanation for this limited agreement could be that a ‘‘collectivity’’ which produces the multi distribution could

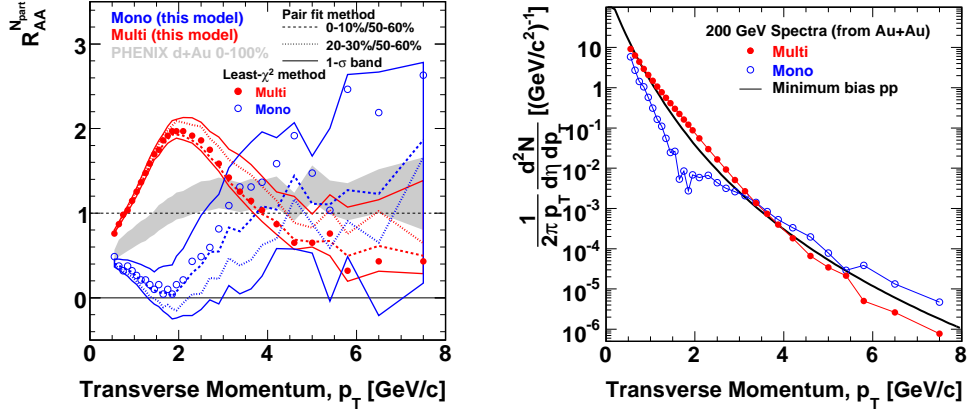


FIG. 10. (color online) Mono and multi nuclear modification factors (scaled by N_{part} not N_{coll}) using the pair fit method on PHENIX, PHOBOS [29], and STAR [30] data. The left panel shows $\sqrt{s_{NN}} = 200$ GeV mono and multi distributions, derived from a fit to the PHENIX data. The dashed and dotted lines show the fits from the centrality bins described in Fig. 9; the outline shows the $1-\sigma$ band, derived from all possible centrality bin pairs. The grey band shows equivalent PHENIX $d+Au$ data [32] from minimum bias collisions for reference. The closed (open) circles represent the results from the least- χ^2 method applied to the spectra (omitting the four lowest centrality points from the fit). The right panel shows the mono and multi spectra using the least- χ^2 fit method. The closed red (open blue) circles represent the multi (mono) collisions spectra per participant. The solid line represents the 200 GeV pp spectra, taken from [28].

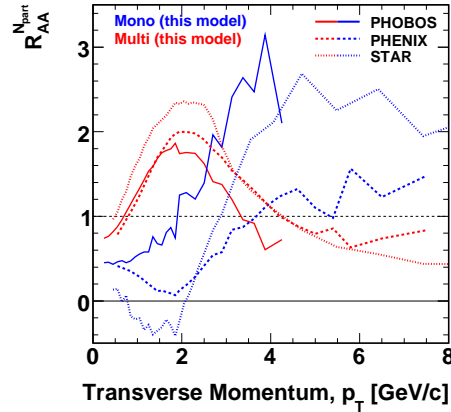


FIG. 11. (color online) Comparison of the mean mono and multi distributions derived from fits to PHOBOS (solid lines), PHENIX (dashed), and STAR (dotted) for Au+Au collisions at 200 GeV.

be dissipating. This could point to a possible need to modify the model to account for an additional scaling variable for example mono, duo and multi ≥ 3 ; this is outside the scope of the current paper.

Figure 10 (left panel) shows the underlying mono and multi nuclear modification factors for $\sqrt{s_{NN}} = 200$ GeV derived from the pair fit method; with the corresponding spectra in the right panel. The dashed and dotted lines represent the centrality bin pairs used in the analysis shown in Fig. 9. The red outline shows a $1-\sigma$ band around the mean underlying multi distribution determined from an average over all possible centrality-pair combinations, except the most peripheral. This appears to be well constrained, illustrating only a small variance in the underlying multi distribution. A comparative analysis using the least- χ^2 method (for the yields versus centrality for each p_T bin) was also performed. (Note that the lowest four centrality points were omitted from the fit.) The results are shown as circles in Fig. 10 (left panel) and are in good agreement with the distributions extracted from the pair fit method. The extracted underlying mono distribution, however, is less constrained, possibly due to a changing surface suppression of mono with centrality. Nonetheless, the extracted values of the mono distributions here are in agreement with the ones obtained from fits to the Au+Au charged particle multiplicity: at very low p_T , a suppression is observed with

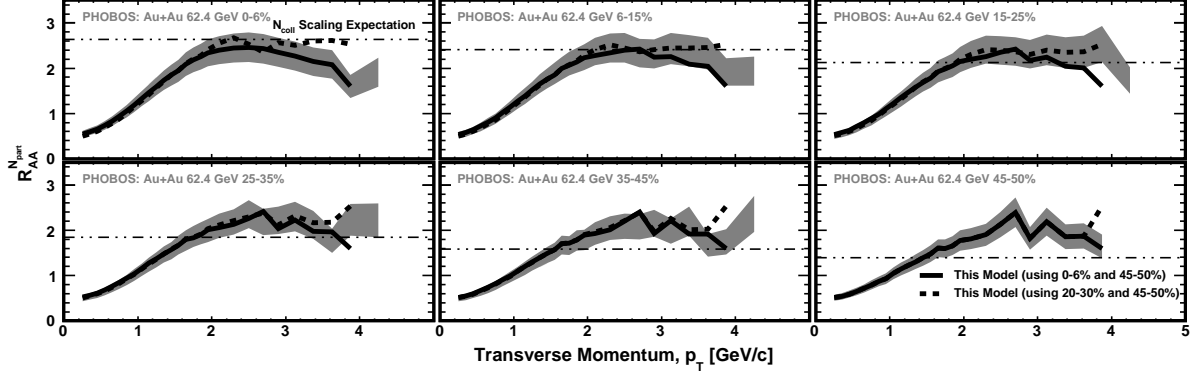


FIG. 12. Nuclear modification factor (scaled by N_{part} not N_{coll}) for unidentified charged hadrons from PHOBOS [33] (filled band) at $\sqrt{s_{\text{NN}}} = 62.4$ GeV. The lines are the $R_{AA}^{N_{\text{part}}}$ reconstituted from the underlying mono- and multi-distributions using the pair fit method; solid (dashed) lines use centrality bins 0-6% (15-25%) and 45-50%. In each figure, the dot-dashed line represents the expected N_{coll} scaling, assuming particle production scales as $pp \times N_{\text{coll}}$.

respect to minimum bias pp collisions. In the intermediate p_T region the mono distribution falls to zero, hinting that the absorption (or suppression) is maximal in this kinematic region. For some fits, it is found that the suppression is ‘negative’ this would represent a case when some additional suppression is present from the edge of the multi-region; pointing, perhaps, toward the need for a mono, duo, and multi ≥ 3 prescription. Figure 11 shows a comparison of the resultant distributions by using PHENIX, PHOBOS [29], and STAR [30] data. The multi distribution in this analysis are found to be very similar. To put the results into context, Fig. 10 shows the multi spectra (per participant) relative to the minimum bias pp spectra, which is found to have the same systematic dependencies as the gluon-dominated system found in Fig. 8. It has been seen that, through the separation into multi and mono sub-components of the collision, a consistent picture can be observed. At the center of this picture is a dense (perhaps gluon dominated) system which is opaque to the particles produced at the periphery of the collision. A gluon-dominated picture is not excluded by other measurements, for example, the anomalous increase of baryons, with respect to mesons, could be expected from a system with a higher number of gluon-jets than quark-jets.

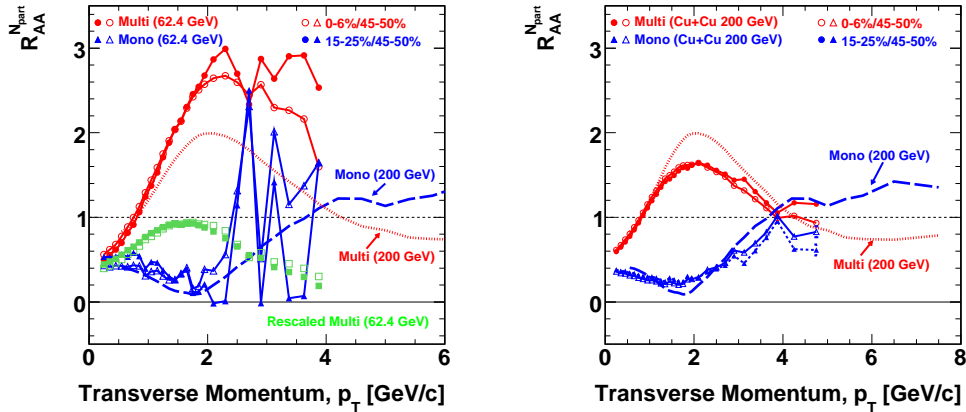


FIG. 13. (color online) The left panel shows the underlying mono (triangles) and multi (circles) $R_{AA}^{N_{\text{part}}}$ distributions for PHOBOS Au+Au data at $\sqrt{s_{\text{NN}}} = 62.4$ GeV [33]. The solid lines are meant to guide the eye. The open (closed) symbols represent a pair fit using centrality bins 0-6% and 45-50% (0-6% and 45-50%). The dashed lines depict the underlying mono and multi distributions from Au+Au collisions at 200 GeV (PHENIX). In order to better compare the multi distributions, the green squares represent the 62.4 GeV data rescaled to the same pp reference (i.e. assumes a 200 GeV pp reference, not 62.4 GeV). The right panel has the same notation as the left, except the data is for PHOBOS Cu+Cu collision data at 200 GeV [34].

It is interesting to note that the disappearance of the away-side jet in two-particle correlations was observed in a

similar p_T region (for the associated particles) as the mono suppression [31]. In this kinematic region, $1 < p_T < 3$ GeV/ c , we find that the underlying mono distribution is very small which perhaps hints that jets are dominantly from the mono (pp -like) interactions which occur on the surface. With this assumption, the away-side is then suppressed (or fully absorbed) within the (multi) medium. At higher p_T , the mono and multi distributions essentially become the same and are similar in magnitude to the measured Cronin-enhanced d +Au data [32]. It should be noted that in order to form these spectral distributions, the N_{coll} scale is explicitly removed. $R_{AA}^{N_{\text{part}}}$ distributions are formed entirely with our participant-like parameters, thus any large-scale suppression in the data (using R_{AA}) is actually brought about by scaling the distributions by N_{coll} . In other words, the suppression at high- p_T could be entirely an artifact of using the wrong scaling variable (namely N_{coll}). How could N_{coll} be the wrong variable? Consider a simple picture. In a standard Glauber model calculation, we assume that each nucleon-nucleon interaction is independent and that the cross-section for each interaction is the same (i.e. σ_{NN} does not change – even after 10 collisions). Once a “collision” has occurred one could surmise that the cross-section is not the same, something has been lost so the cross-section could be diminished. Further, if one assumes that the multi component melts into a single (not discrete) system, then it may be impossible, in fact improbable, to manifest multiple collisions, or at least reliably count them. Note that, experimentally, one cannot count N_{coll} , yet one can directly count N_{part} , or at least derive it from the data with some certainty.

It has already been observed that by dividing the $\sqrt{s_{\text{NN}}} = 200$ GeV charged hadron spectra by that from 62.4 GeV, the ratio (for a given p_T) is invariant across all centrality bins measured [27]. This may already indicate a simple geometry scaling which factorizes in energy and centrality. We should therefore expect a similarly successful fit using the mono/multi approach for 62.4 GeV data. Fig. 12 shows the same analysis using PHOBOS charged hadron spectra at $\sqrt{s_{\text{NN}}} = 62.4$ GeV [33], where two centrality bin pairs can be used to predict all other bins. Fig 13 shows the resultant mono distribution, illustrating the same level of suppression as 200 GeV, whereas 62.4 GeV has a higher multi $R_{AA}^{N_{\text{part}}}$. In the calculation of $R_{AA}^{N_{\text{part}}}$, the pp spectrum is used in the denominator to observe any differences between A+A and pp collisions. To more fairly compare the two spectra, the green squares represent the same 62.4 GeV data, but rescaled to effectively use the pp 200 GeV reference. In this way, we see that the underlying multi spectrum grows with energy. A similar rescaling of the underlying mono distribution is not performed as for that case, the relative change to pp is important, not the overall spectrum. It is interesting to note that $R_{AA}^{N_{\text{part}}}$ for mono-collisions is the same for 200 GeV and 62.4 GeV. This indicates that the level of suppression does not depend on collision energy (at least for these RHIC energies).

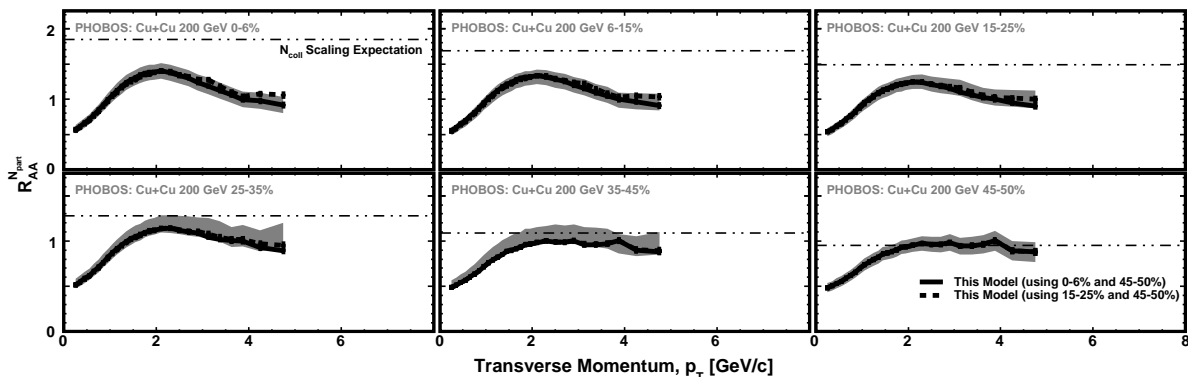


FIG. 14. Nuclear modification factor (scaled by N_{part} not N_{coll}) for unidentified charged hadrons from PHOBOS (filled band) in Cu+Cu collisions at $\sqrt{s_{\text{NN}}} = 200$ GeV [34] and from the model fit using the pair fit method (lines). For the solid lines, the centrality bins 0-6% and 45-50% were used, dashed lines used centrality bins 15-25% and 45-50%.

In the multiplicity analysis, we tested the hypothesis that common underlying distributions for the Au+Au and Cu+Cu data can be used to represent the data. It is possible to also perform the same comparisons with the unidentified charged hadron spectra. In Fig. 14, a pair-fit using PHOBOS Cu+Cu data at $\sqrt{s_{\text{NN}}} = 200$ GeV [34] is invoked to extract the underlying mono- and multi-distributions, which are then used to reconstitute the $R_{AA}^{N_{\text{part}}}$ in Cu+Cu for each centrality bin. In contrast, Fig. 15 uses the underlying mono- and multi-distributions derived from Au+Au collisions to form the $R_{AA}^{N_{\text{part}}}$ for each centrality bin. In both cases, a reasonable fit is found. For completeness, the right panel in Fig. 13 shows a comparison between the underlying mono and multi distributions from Au+Au

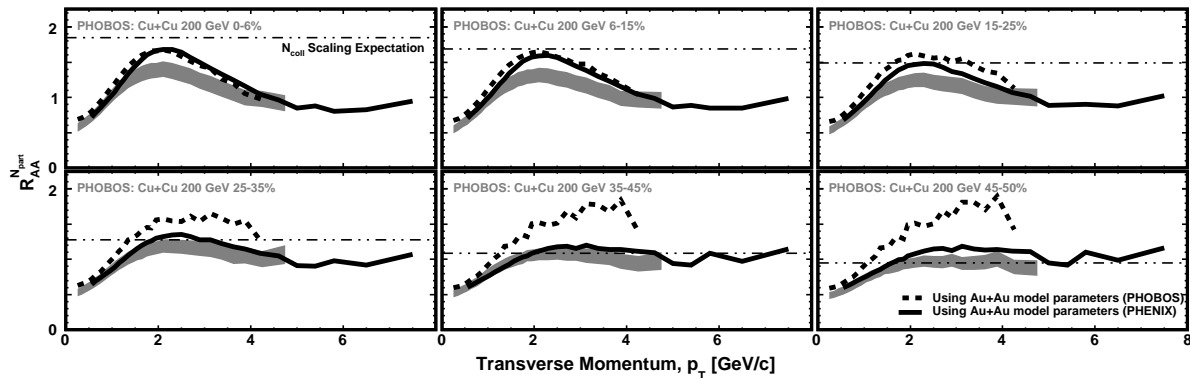


FIG. 15. Nuclear modification factor (scaled by N_{part} not N_{coll}) for unidentified charged hadrons from PHOBOS (filled band) in Cu+Cu collisions at $\sqrt{s_{\text{NN}}} = 200$ GeV using the model fit results for the mono and multi distributions from the Au+Au analysis. The dashed (solid) lines use the results from fitting the PHOBOS (PHENIX) data.

(symbols) and those derived from Cu+Cu (lines). The two sets of symbols for Cu+Cu represent the pair fit method using PHOBOS centrality bins 0-6% and 45-50% (open symbols) and 0-6% and 45-50% (closed symbols).

FREEZE-OUT PROPERTIES

As an extension to the low- p_T particle studies, it has proven useful to fit the resultant spectra with models to derive freeze-out properties of the system. Commonly, the kinetic freeze-out temperature (T_{kin}) and radial flow velocity (β) of the system are derived from a Blast-wave [35] fit to the low- p_T spectra of identified pions, kaons, and protons. For a description see for example Refs. [36, 37]. At kinetic freeze-out all elastic collisions cease and the spectral shape is fixed. The extracted parameters reflect the state of the system at that time. What has been observed, through the Blast-wave fits, is that T_{kin} and β vary quite strongly as a function of centrality. Here, we address the question whether those results can be described within the mono/multi framework. In a similar way to the above analysis, we consider that mono and multi have their own “universal” T_{kin} and β values. Using the least- χ^2 method described above, we fit the centrality dependence of the freeze-out variables and extract those parameters (Y variables in Eqn.1) for mono and multi. The left and right panels of Fig. 16 shows the result of fitting the freeze-out temperature (T_{kin}) and radial flow velocity (β), respectively, at $\sqrt{s_{\text{NN}}} = 200$ and 62.4 GeV from STAR [36]. From the fits we find that the centrality dependence is well described in this framework, and the extracted T_{kin} and β values for the underlying mono and multi components are given in Table II. Although there is some collision energy dependence, the more striking feature is that the mono results for T_{kin} and β are significantly different from the multi values. A consistent picture emerges that the multi component has considerably larger β values and a freeze-out temperature of about one-half of that of the mono.

Figure 17 shows the results of a comparative analysis using the freeze-out parameters from Cu+Cu collisions at STAR [37]. Differences between Au+Au and Cu+Cu evident, especially at the highest energy. The heavier Au+Au system has a larger β and smaller T_{kin} than those extracted from Cu+Cu collisions, see Fig. 17. Although there are differences, we did not consider the systematic uncertainties in the data when creating the underlying distributions for the two collision systems, so it becomes difficult to draw any strong conclusions. In comparison to the freeze-out parameters extracted for pp collisions, for Au+Au collisions at 200 GeV, the extracted T_{kin} for the underlying mono component is about 25% higher than that from the corresponding pp value (0.127 ± 0.013 [36]). Similarly, the extracted radial flow velocity is about 35% lower than the corresponding pp value (0.244 ± 0.081 [36]). We should note here, that we do not expect the mono to be precisely as minimum bias pp . In particular, the extracted underlying mono distributions for multiplicity and charged hadron spectra are different from minimum bias pp , especially in the low- p_T region.

From this analysis, if we take the Blast-wave model at face value, it appears as though the kinetic freeze-out of the mono collisions, around the surface, occurs earlier than the multi, as implied by the different temperatures at freeze-out. This, in turn, suggests that the kinetic freeze-out occurs at a later time such that elastic collisions still occur in the multi after the complete freeze-out of the mono. The radial velocity, β , is found to be far greater for the

multi, possibly indicating a more explosive expansion. Thus, one could argue that the multi system is simply more densely compact. We note that, the Blast-wave fits are simply reflecting the difference between the underlying mono and multi spectral shapes.

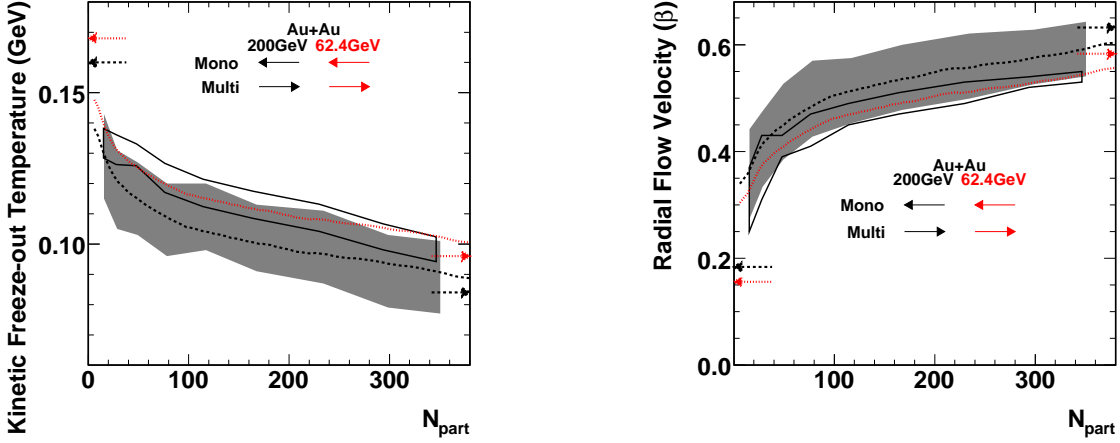


FIG. 16. (color online) Least- χ^2 fit to the kinetic freeze-out temperature (left) and radial flow velocity (right) for Au+Au collisions at 200 (filled band) and 62.4 GeV (outline band). Dashed (dotted) lines represent the 200 GeV (62.4 GeV) fit results. The left (right) pointing arrows depict the mono (multi) T_{kin} or β in each panel.

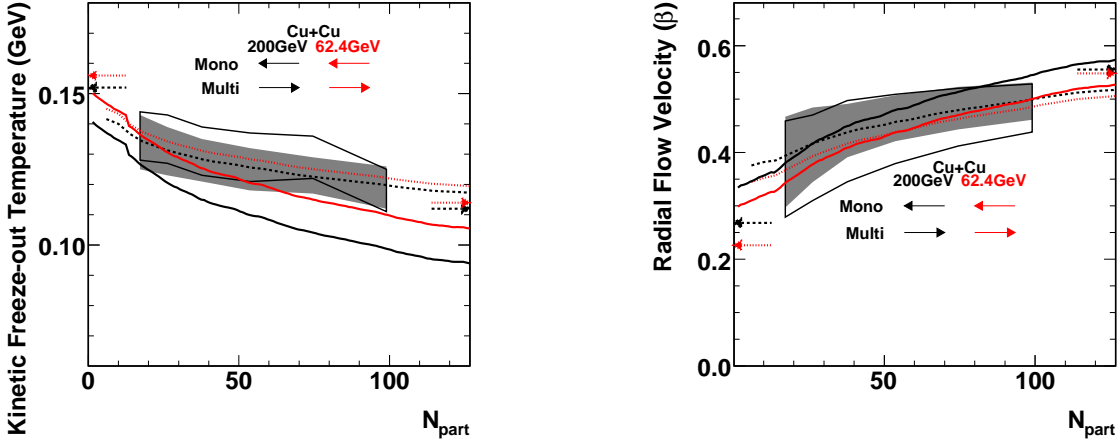


FIG. 17. (color online) Least- χ^2 fit to the kinetic freeze-out temperature (left) and radial flow velocity (right) for Cu+Cu collisions at 200 (filled band) and 62.4 GeV (outline band). Dashed (dotted) lines represent the 200 GeV (62.4 GeV) fit results. The left (right) pointing arrows depict the mono (multi) T_{kin}/β .

In the evolution of the collision, a chemical freeze-out occurs prior to the kinetic freeze-out. Chemical freeze-out occurs once all inelastic collisions have ceased; freezing the particle species. It is found that this temperature (T_{ch}) is invariant with centrality [37], thus both the mono and multi must have the same apparent chemical freeze-out temperature.

SUMMARY

In summary, we have shown that some aspects of heavy ion data can be reproduced using a simple two-component model, with participant-like scaling variables. As an initial test of the model, we find that the multiplicity and

TABLE II. Mono and multi freeze-out parameters as derived from the least- χ^2 fit to the mid-rapidity data from STAR.

Energy (GeV)	Au+Au				Cu+Cu			
	mono		multi		mono		multi	
	T_{kin} [GeV]	β	T_{kin} [GeV]	β	T_{kin} [GeV]	β	T_{kin} [GeV]	β
200	0.160	0.163	0.084	0.639	0.152	0.268	0.112	0.555
62.4	0.168	0.184	0.096	0.576	0.156	0.226	0.114	0.548

unidentified charged hadron spectra can be reproduced with an underlying gluon-dominated distribution; the latter without the need for a large suppression at high- p_T . By fitting the data, we can simultaneously extract underlying distributions for each sub-component of the collision: the singly-hit mono participants and the multiply-hit multi. From this, a suppression is observed, however, it is limited to particles originating at surface-collisions (mono) and mostly in the low- to intermediate- p_T region. The component characterizing the multiple nucleon-nucleon interactions is found to be peaked in the intermediate p_T region and becomes flat at the highest measured p_T . With these two sub-components, we observe that there is a mechanism by which one can reliably reproduce the multiplicity, spectral shapes, and freeze-out parameters. There is no need for a large (up to a factor of five) suppression which is currently used to describe the heavy ion data using the N_{coll} variable. At the center of this model picture is a dense (perhaps gluon dominated) system (multi) which is opaque to the particles produced at the periphery of the collision (mono). A gluon-dominated picture is not excluded by other measurements, as discussed, the anomalous increase of baryons, with respect to mesons, could be expected from a system with a higher number of gluon-jets than quark-jets, though more details are outside the scope of the current paper.

To conclude, in our model, we assert that the yield of high- p_T particles is not suppressed. The apparent reduction in yields observed at high- p_T is in fact due to a different particle production mechanism than what is expected from minimum bias pp interactions. In particular this mechanism does not produce high- p_T particles at the expected binary collision rate, but rather at a slower rate as determined by the geometry of the collision, in a similar way to that expected from close-packed gluons.

This work was partially supported by US DOE Grants DE-FG02-04ER41325, DE-FG03-86ER40271, and DE-FG02-94ER40865.

-
- [1] M.Basile *et al.*, Phys. Lett. **B95** (1980) 311.
[2] B.B.Back *et al.*, Phys. Rev. **C74** (2006) 21902(R).
[3] R.S.Hollis, Ph. D. Thesis, University of Illinois at Chicago (2005).
[4] R.J.Glauber, in Lectures in Theoretical Physics, edited by W.E.Brittin and L.G.Dunham (Interscience, N.Y.), Vol.1, 315 (1959).
[5] K.Werner, Phys. Rev. Lett. **98** (2007) 152301.
[6] J.Aichelin and K.Werner, Phys. Rev. **C79** (2009) 064907.
[7] B.Alver *et al.*, arXiv:0805.4411v1[nucl-ex].
[8] T.Sjöstrand *et al.*, Comput. Phys. Commun.,**178** (2008) 852. PYTHIA version 8.108 is used.
[9] M.Gyulassy and X.N.Wang, Phys. Rev. **D44** (1991) 3501.
[10] Z.Tang *et al.*, arXiv:1101.1912v2[nucl-ex].
[11] M.Gyulassy and X.N.Wang, HIJING, Comput.Phys.Commun **83** (1994) 307.
[12] D.Kharzeev and M.Nardi, Phys. Lett **B507** (2001) 121.
[13] S.S.Adler *et al.*, Phys. Rev. Lett. **94** (2005) 232301.
[14] K.Reygers *et al.*, J. Phys. G **35** (2008) 104045
[15] J.Adams. *et al.*, Phys. Rev. Lett. **97** (2006) 162301.
[16] B.B.Back *et al.*, Phys. Rev. Lett. **91** (2003) 052303.
[17] A.Bialas *et al.*, Nucl. Phys. **B111** (1976) 461.
[18] B.B.Back *et al.*, Phys. Rev. Lett. **87** (2001) 102303.
[19] B.B.Back *et al.*, Phys. Rev. **C74** (2006) 021901(R).
[20] B.Alver *et al.*, Phys. Rev. Lett. **102** (2009) 142301.
[21] G.J.Alner *et al.*, Z. Phys. **C33** (1986) 1.
[22] W.Thome *et al.*, Nucl. Phys, **129** (1977) 365.
[23] B.B.Back *et al.*, Phys. Rev. **C65** (2002) 061901(R).
[24] B.B.Back *et al.*, Phys. Rev. **C65** (2002) 031901(R).
[25] B.B.Back *et al.*, Phys. Rev. **C70** (2004) 021902(R).
[26] K.Aamodt *et al.*, Phys. Rev. Lett **106** (2011) 032301.

- [27] B.Alver *et al.*, Phys. Rev. **C80** (2009) 011901(R).
- [28] S.S.Adler *et al.*, Phys. Rev. **C 69** (2004) 034910.
- [29] B.B.Back *et al.*, Phys. Lett. **B578** (2004) 297.
- [30] J. Adams *et al.*, Phys. Rev. Lett. **91** (2003) 172302.
- [31] C.Adler *et al.*, Phys. Rev. Lett. **90** (2003) 082302.
- [32] S.S.Adler *et al.*, Phys. Rev. Lett. **91** (2003) 072303.
- [33] B.B.Back *et al.*, Phys. Rev. Lett. **94** (2005) 082304.
- [34] B.Alver *et al.*, Phys. Rev. Lett. **96** (2006) 212301.
- [35] E.Schnedermann *et al.*, Phys. Rev. **C48** (1993) 2462.
- [36] B.I.Abelev *et al.*, Phys. Rev. **C79** (2009) 34909.
- [37] M.M.Aggarwal *et al.*, 1008.3133[nucl-ex].